NTNU

Norwegian University of
Science and Technology

Cuttings Bed Erosion in Horizontal Wells

Hugo Alexandre Machado
Ganga

Petroleum Engineering
Submission date: June 2016
Supervisor: Pål Skalle, IPT
Co-supervisor: Benjamin Werner, IPT

Norwegian University of Science and Technology
Department of Petroleum Engineering and Applied Geophysics

Hugo Alexandre Machado Ganga

Cuttings Bed Erosion Threshold In Horizontal Wells

Trondheim, June,2016

NTNU Norwegian University of Science and Technology
Faculty of Engineering Science and Technology
Department of Petroleum Engineering and Applied Geophysics

Acknowledgement

This thesis as been carried out at the Department of Petroleum Engineering and Applied Geophysics at NTNU, Norway under the supervision of Professor Pål Skalle and Mr. Benjamin Werner.

I would like to thank both Professor Pål Skalle and Mr. Benjamin Werner for the supervision during the process.

Summary

Many of the time consuming and economically demanding drilling problems faced today can be tracked back to poor hole cleaning, even more so when drilling through highly inclined sections. Improved hole cleaning operations can subsequently guarantee improved well construction quality.

Hole cleaning has been subjected to comprehensive investigation, where “rules of thumb” have been proposed to ensure acceptable levels of cuttings transport to surface. Nonetheless, the superiority of oil based muds over water based muds is still not fully understood.

To try and unveil the ambiguities within the topic, this thesis focuses on the erosion threshold of cuttings beds where a simple model and laboratory experiments methodology to be followed are proposed. Instead of the standard approach taken to this date in the petroleum engineering field, where most of the efforts are directed into the drilling fluids features, here we follow the sedimentology’s approach, where both drilling fluid and cuttings bed composition are thoroughly reviewed.

Table of Contents

List of Figures

List of Tables

1 Introduction

Due to the oil and gas industry economic demands and targets, the majority of wells drilled require lengthier and lateral highly inclined displacement paths. One of the major problems associated with operations in highly inclined wells is achieving appropriate cuttings transport to surface.

During drilling operations, the cuttings settling direction for highly inclined (horizontal) wells is still vertical, although they will settle in a much shorter period of time due to the smaller length needed to reach the annular wall. This leads to a diminished vertical velocity component fluid, hence, the drilling mud's capability of suspending the cuttings reduces greatly, turning cuttings bed accumulation in the borehole into an inevitable process. Field experience has shown that oil base muds (OBM) are better than water base muds (WBM) when it comes to wellbore cleaning applications, but the reasons behind this phenomenon are still not well understood.

Cuttings transport is a thoroughly investigated subject, as opposed to the erosion and erosion threshold of cuttings bed, nonetheless within the work done on these subjects, most of the efforts focused on the effects of fluid rheological and hydraulic properties with no special attention into the cuttings bed composition physical quantities.

To counteract these facts, this thesis looks at presenting a new way of looking at the erosion threshold of a cuttings bed problem by following the sedimentology's approach, where both the fluids and the cuttings bed composition properties are considered. This is achieved by reviewing and analyzing the main physical quantities involved in the erosion threshold problem so that a basic model relating the erosion threshold condition to a set of meaningful non-dimensional expressions can be obtained. Finally a laboratory experiment method is also proposed, so that the influence of the different non-dimensional expressions affecting the erosion threshold of a cuttings bed can be analyzed.

2 Previous Related Work

Most of the work in the oil industry comparing OBM to WBM has been focused on the efficiency of cuttings transport to surface, and little to no attention has been given to the role of the cuttings bed composition. However, there are some studies where the cuttings bed physical quantities are also taken into account when evaluating erosion.

Cuttings bed composition plays a more significant role in erosion studies for varies other fields, such as agriculture and civil engineering, where factors such as particle grain size and cuttings clay content form part of the physical quantities being considered. This section will provide an insight into some of the work done within and outside the oil industry, and the main conclusions achieved by researchers.

Nance (1983) made one of the earliest comparisons, were the efficiency of both drilling fluids (oil based and water based muds) were tested for 6 wells in the Gulf of Mexico. He noticed that OBM would prove to be much better at cleaning the hole and avoiding hole cleaning problems than WBM when drilling through zones of expected concern. Special recommendations were made for those troubled segments with inclinations higher than 30° and for holes with 12-1/4'' ID or more, where satisfactory hole cleaning can only be achieved when OBM can be pumped at annular velocities of 150ft/min or higher.

Although his work compared the efficiency of WBM vs. OBM when cuttings are being transported to surface, it made no remarks on the erosion of the cuttings process. To account for this effect, most of the work done took only WBM into consideration. Adari (2000) published a paper where the optimum drilling fluid properties and flow rates are determined in order to minimize both cuttings bed height and the circulation time for high angled wells and he concluded that:

- Cuttings bed erosion occurs at faster rates for higher fluid flow rates
- For a given fluid flow rate, cuttings bed height is reduced when viscosity of the fluid is also reduced
- Cuttings removal is easier with turbulent flow rather than laminar flow
- Cuttings accumulation in a well increase with the increased angle of the well

Ramadan (2001), also published one study where a solid bed erosion model in combination with the cuttings transport mechanistic model is used to analyse the forces acting on a solid bed particle and to estimate the removal rate of a solid particle from the surface of a solid bed. He developed a simple lab test flow loop to compare it against model predictions, and evaluated the cuttings erosion rate against particle size and annular flow rates. He concluded that:

- His model predictions and experimental results confirmed a direct relationship between particle acceleration and particle size

- Results showed that both rolling and lifting of bed particles, caused by drag and lift forces exist simultaneously during solid bed erosion; however, one mechanism may dominate the other, depending upon angle of inclination, flow velocity and viscosity of the fluid
- When transporting solid particles and cuttings there is an optimum particle size that has the highest rate of removal

Hong (2008) published a study on the erosion threshold of a granular bed driven by laminar fluid flow as a function of particle grain size and roughness. He noted that bed armouring and grain size are major influences in the erosion threshold, and the bed preparation also showed major influences in the values obtained as the armouring of the bed may be more related to the relative arrangement of the grains at the surface than the size sorting of the cuttings bed.

While these results prove to be of use for this thesis when it comes to the erosion evaluation of granular beds, they fall short when clay content is introduced to the system. Due to their complex interactions with the medium fluid, cohesive beds introduce new challenges to the task. Heizen (1976) stated that for cohesive soils, the "erodability" is generally a function of:

- Amount and type of clay present in the clay fraction
- Chemical composition of the pore fluid
- Presence of organic matter and other cementing agents
- Particle grain size
- Thixotropic and stress history of the soil matrix
- Temperature, pH and water content of the soil matrix

3 Cuttings Bed Erosion and Erosion Threshold Principles

This chapter will provide the basic knowledge required for the understanding of the erosion and erosion threshold of cuttings bed processes. This will be achieved through the following steps:

- A description of the fluid flow main physical quantities and their uncertainties
- Cuttings bed main physical quantities and behaviours
- Definition and the main physical quantities of erosion and erosion threshold of a cuttings bed

With this in mind, it is reasonable to say that both erosion and erosion threshold of a cuttings bed will be dependent on fluid flow, cuttings bed and the system (acceleration of the gravity, g) physical quantities, as given by equations (1) and (2):

$$Erosion = f(Fluid\ flow\ parameters, Cuttings\ Parameters, g) \quad (1)$$

$$\begin{gathered} Erosion\ threshold \\ = f(Fluid\ flow\ parameters, Cuttings\ bed\ parameters, g) \end{gathered} \quad (2)$$

3.1 Fluid Flow

Inevitably, fluid density, ρ_f, and fluid viscosity, μ, are two vital properties used to describe fluid properties. Apart from those two logical choices, the fluid flow strength is the other parameter that strongly influences both the erosion and erosion threshold of a cuttings bed, and it can normally be represented as shear stress, τ, and or mean fluid velocity, U.

For an open channel flow, under steady uniform conditions (where cross section does not vary with time and space), Newton's second law can be used to derive an expression for the boundary shear stress, τ_0, under laminar fluid flow conditions. At a first glance of this problem, the channel is assumed to have an infinite width with no side boundaries (a rectangular cross section channel flow with flow width much larger than the flow depth is a good approximation of this statement) as shown in figure (1).

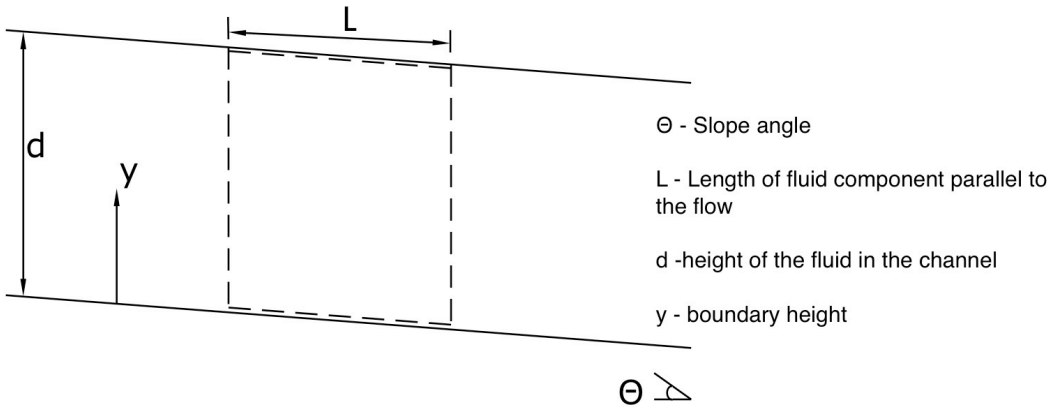

Figure 1: Definition sketch for deriving boundary shear stress in a steady uniform flow

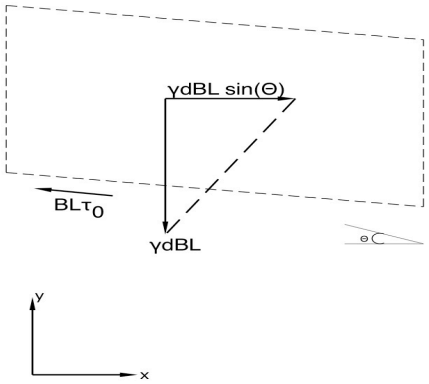

γ = Fluid component specific weight

d = Fluid flow height

B =Width of fluid of the channel

L = Length of fluid component parallel to the flow

Θ = Channel inclination

τ_0=Boundary shear stress

Figure 2: Fluid component free body diagram

Writing Newton's second law for the fluid free body diagram showed in figure (2), the balance of forces in x-axis is given by:

$$\gamma dBL sin\Theta = \tau_0 BL \tag{3}$$

Solving for the boundary shear stress one obtains:

$$\tau_0 = \gamma\, d\, sin\Theta \tag{4}$$

For a rectangular cross section case with a given width, b, equation (4) can be re-written as:

$$\tau_0 = \gamma\, sin\Theta\, \frac{bd}{2d+b} \tag{5}$$

Both shear stress and velocity at all points in the flow can also be found by applying the same force balance principle to the fluid free body diagram and are normally expressed as:

$$\tau = \tau_0 \left(1 - \frac{y}{d}\right) \tag{6}$$

$$u = \frac{\gamma sin\alpha}{\mu}\left(yd + \frac{y^2}{2}\right) \tag{7}$$

By the non-slip condition, fluid velocity is known to be zero at the bottom of the flow (y=0), hence, it is only reasonable to assume that the same velocity must increase upward in the flow. Both the shear stress and the velocity gradient display a linear distribution profile, from a zero value at the surface to a maximum value at the boundary.

Figure (3) illustrates the profiles for fluid shear stress, velocity and velocity gradient in a steady uniform laminar open channel flow. Note that the forces exerted at the free surface (interface between air and fluid) are here neglected.

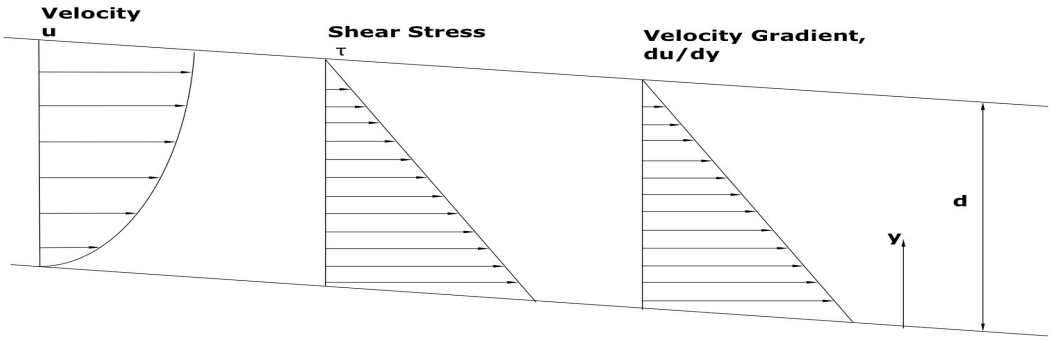

Figure 3: Velocity, shear stress and velocity gradient profiles in laminar open channel flow

As long as the flow remains steady and uniform on average, the linear distribution of shear stress from zero at the surface to a maximum value at the boundary should hold true even for turbulent fluid flow cases. This is not true for the velocity profile, as the shear stress across a shear plane is different in turbulent flow due to the influence of turbulent shear stress. Figure (4) shows how the velocity profile varies from laminar to turbulent flow cases in open channel flows.

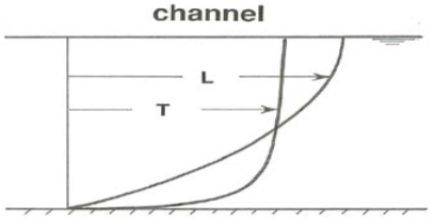

Figure 4: Laminar (L) and turbulent (T) flow velocity profile for open channel flow (from Southard, John. *12.090 Special Topics: An Introduction to Fluid Motions, Sediment Transport, and Current-generated Sedimentary Structures, Fall 2006)*

3.1.1 Turbulent Shear Stress

Turbulent flow has a significant effect in the transport of suspended material, where instead of a straight trajectory, particles follow a sinusoidal trajectory and their velocity is irregular rather than constant. Normally they undergo two types of accelerations at the same time:

- Temporal accelerations: because the velocity varies with time at points the particle happens to occupy
- Spatial accelerations: because the particle falls through regions with different fluid velocity

During turbulent fluid flow the total shear stress across the shear plane is the sum of the turbulent shear stress (caused by macroscopic diffusion of fluid momentum) and the viscous shear stress (caused in part by molecular diffusion of fluid momentum and in part by the attractive forces between molecules at the shear plane). Assuming that the boundary is physically smooth, 3 qualitatively different but intergrading zones of flow can be recognized, as shown in figure (5).

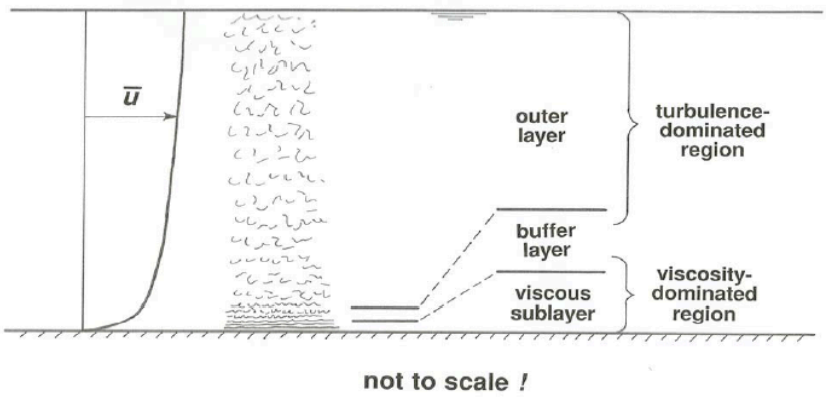

Figure 5: Flow zones (from Southard, John. *12.090 Special Topics: An Introduction to Fluid Motions, Sediment Transport, and Current-generated Sedimentary Structures, Fall 2006)*

The viscous sub-layer is a thin layer closest to the boundary in which the viscous shear stress dominates over the turbulent shear stress. The thickness of this layer depends on the characteristics of the particular flow and fluid. In the case of physically smooth boundaries the thickness of the layer is easily defined, but if the boundary is covered with closely spaced roughness elements with heights greater than the thickness of the viscous sub-layer, this sub-layer ceases to exist and the turbulence extends all the way to the boundary.

The buffer layer is a zone where both viscous and turbulent shear stresses play a major role. This is a fairly thin layer (still thicker than the viscous sub-layer), where part of the turbulence generated is carried outward into the outer layer and part is carried inward into the viscous sub-layer. Finally, the outer layer is

the one that occupies most of the flow and extends all the way to the surface and is completely dominated by turbulent shear stress.

3.1.2 Forces exerted by the Fluid Flow on the Boundary

At every point on the solid boundary two kinds of fluid forces act:

- Pressure acting normal to the local solid surface at the point
- Viscous shear stress acting tangential to the local solid surface at the point

For smooth boundaries, the downstream component of fluid forces on the boundary can only result from the action of the viscous shear stress, this because the pressure forces have no component in the direction of the flow. On the other hand, if the boundary is rough (uneven), because there's a downstream component of the pressure forces on the boundary in addition to the downstream component of the viscous forces, local pressure forces are greater on the upstream sides than on the downstream sides, hence, each element is subjected to a resultant pressure force with a component in the downstream direction, as shown in figure (6).

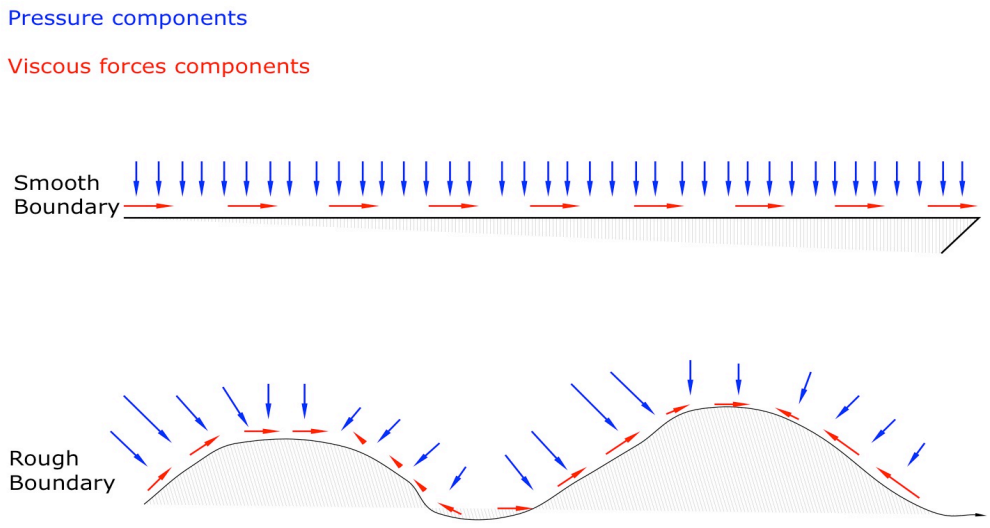

Figure 6: Pressure and viscous forces components in smooth and rough boundaries

The details of pressure on rough beds are complicated and not here discussed, as they depend on the boundary Reynolds number (Reynolds number based on the size of the roughness elements), the local velocity of the flow around the roughness elements, as well as shape, arrangement and spacing of these same elements. However, as a general rule, figure (7) demonstrates how pressure varies in rough boundaries.

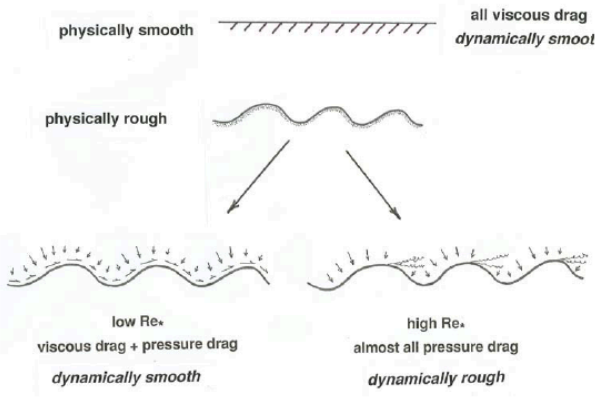

Figure 7: Rule of thumb for pressure variance in smooth and rough boundaries (from Southard, John. *12.090 Special Topics: An Introduction to Fluid Motions, Sediment Transport, and Current-generated Sedimentary Structures, Fall 2006)*

Due to this uneven distribution of forces in rough beds, only a small part of the boundary shear stress will represent the boundary friction that is directly responsible for particle motion. The rest is the form drag on the main roughness elements; hence, shear stress can be as erratic as the mean velocity (recall that the velocity profile is different in laminar and turbulent flows), as shown in figure (8).

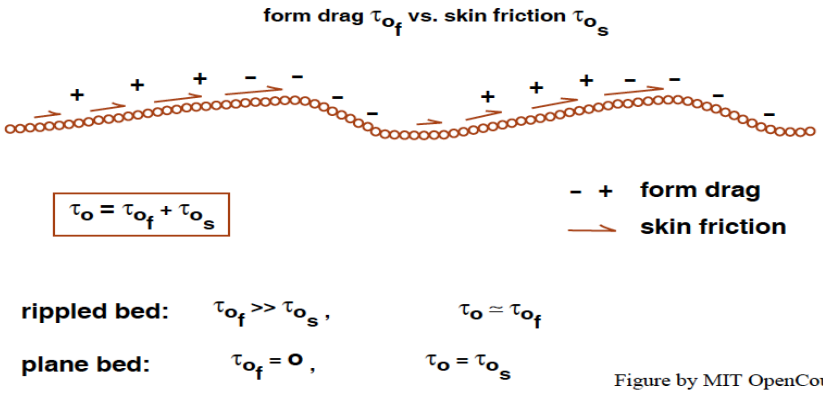

Figure by MIT OpenCourseWare.

Figure 8: Boundary shear stress in rough boundaries (from Southard, John. *12.090 Special Topics: An Introduction to Fluid Motions, Sediment Transport, and Current-generated Sedimentary Structures, Fall 2006)*

When uneven boundaries are presented, the spatially and temporally local skin friction would be the best variable to describe the erosion and erosion threshold processes, but the problem is that it cannot be measured, and it can only be estimated with considerable uncertainty using drag partion approaches.

3.2 Cuttings Bed

Figure (9) shows a bed of loose particles submerged in a fluid, where the zone of interest for this study lies in the upper part of the bed (the active layer), a zone where the particle movement is strongly affected by the fluid flow.

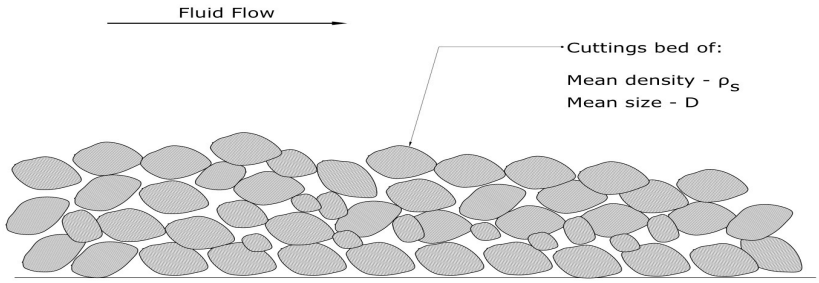

Figure 9: Cuttings bed

A mean size (median diameter), D, shape, and mean density, ρ_s, are normally used to characterize the cuttings bed, but normally due to the many uncertainties within the exact shape of the particles, here we focus solely on the density and size of the particles.

All sediments have a range of particle sizes, and the spread of sizes around the average size is called sorting, which is here represented as σ. As shown in figure (10), a well sorted cuttings bed shows a narrow spread of sizes while a poorly sorted cuttings bed shows a wide spread of sizes.

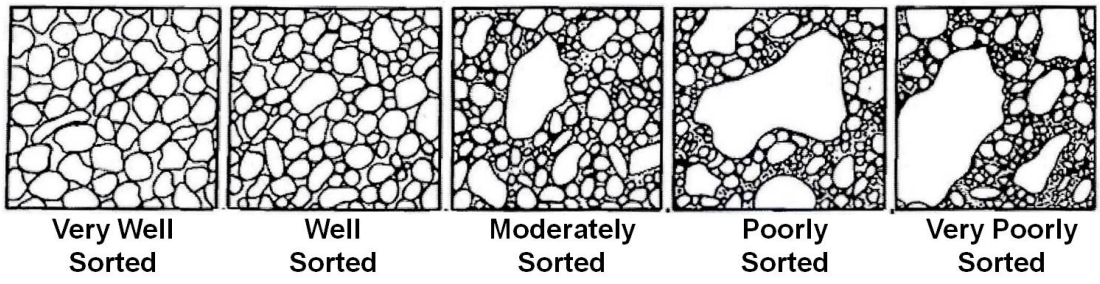

Figure 10: Cuttings sorting (The Rainbow of Rodeo Beach. (n.d.). Retrieved Juned 24 2016, from https://www.geocaching.com/geocache/GC2H5H8_the-rainbow-sands-of-rodeo-beach?guid=1f62114-c0ae0474b0871d-459498b5eba7)

Also important to take into consideration are the parameters that describe the effects of cohesive particles. Cohesion has is origins on electro-chemical forces, and the magnitude of these forces depends on the mineralogy (e.g. exchangeable cations), size and shape of the cohesive particles, spatial arrangement of the clay particles and the ionic properties of the pore and eroding fluid. Also, the resistance properties depend on the state and history of consolidation (e.g. compacted and dry clays are harder to erode than soft wet clays), and although not always considered the microbial organisms also have an important effect on the cohesion.

When cohesive particles are added into the system, grain size and density are normally not enough to describe erosion and erosion threshold problems. Various studies have been performed relating the effects of cohesive particles on the erosion and erosion threshold of a cuttings bed, and the list of variables chosen to describe the effects of cohesion vary from study to study.

3.2.1 Cuttings Transport Modes

The aggregate of cuttings being transported by the flow (all the particles in motion in a given flow whether or not they are in contact with the cuttings bed) is called the load. Layer refers to all the particles that at a given time are motionless and in contact with the cuttings bed. The flow is defined as all the material (fluid and solid) that at a given time is in motion above the cuttings bed.

The load can be further divided into:

- Bed material load: part of the load who's size is represented in the cuttings bed
- Wash load: part of the load that's not represented in the cuttings bed
- Bed load: part of the load that travels in direct contact with the cuttings bed
- Suspended load: part of the load that is maintained temporarily in suspension above the cuttings bed by the action of upward moving turbulent eddies (likely to be partly bed material load and partly wash load)

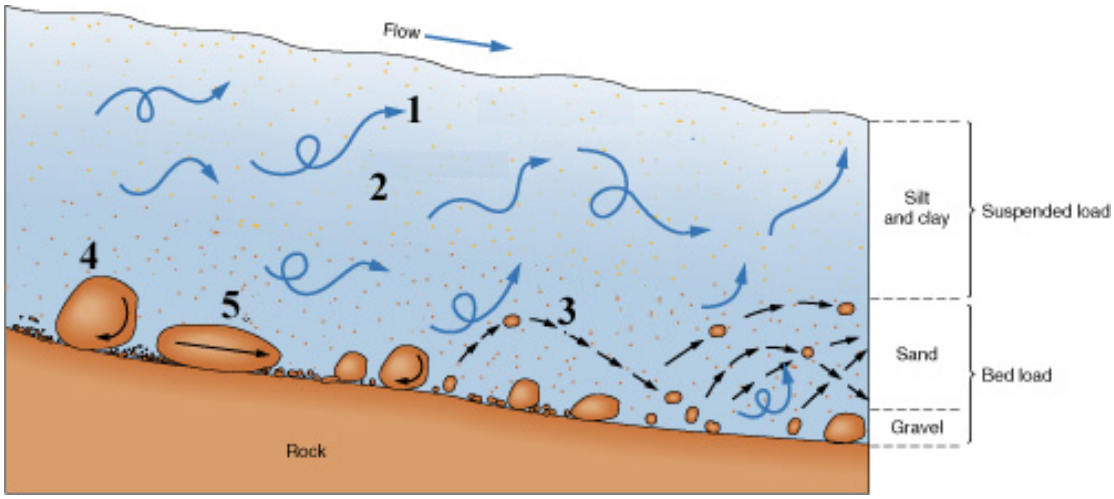

Figure 11: Cuttings transport modes (from Assignment Material - PlantItWeb Homepage. (n.d.). Retrieved June 24, 2016, from http://www.ih2000.net/kemoffatt/acct_2301_finc/Williams-12th Chapter 3/18-Assignment Material.mht)

At weak fluid flow strengths, where the particle motion is neither continuous nor uniform over the cuttings bed, the particles start moving as bed load. As the flow strength increases some of the particles near the bed are lifted by the upward moving turbulent eddies and travel for more or less long distances downstream as suspended load. As a general rule, the stronger the fluid flow is and/or the

finer the particles are, the greater is the concentration of suspended load and the higher it can travel downstream in the flow before returning to the bed.

If small sized clay particles are introduced into the system, they would travel in suspension, but the main difference with the suspended load is that even if added in large quantities they will not be represented (visible) in the cuttings bed, hence, those are characterized as wash load.

3.2.2 Cuttings Bed Configurations

Granular bed configurations made by unidirectional flows have been well studied, and in the case of well-sorted granular cuttings bed they normally present the sequence shown in figure (12).

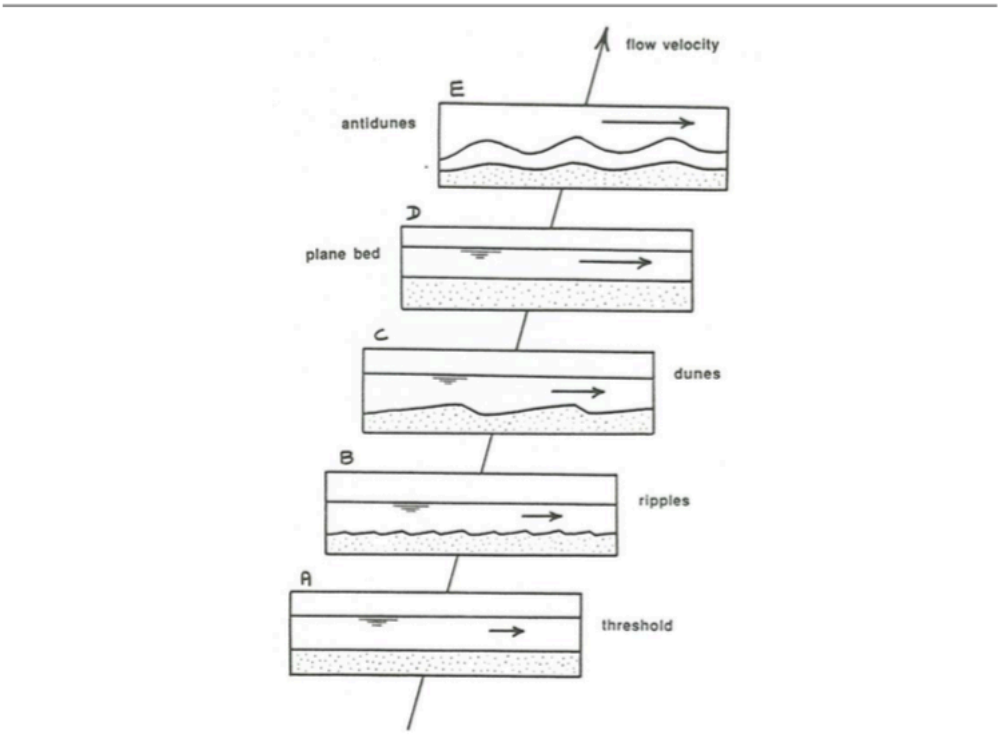

Figure 12: Bed configurations for medium sand at increasing fluid flow velocities for open channel flow (from Southard, John. *12.090 Special Topics: An Introduction to Fluid Motions, Sediment Transport, and Current-generated Sedimentary Structures, Fall 2006)*

As the erosion threshold condition it's exceeded, as shown in figure (12-A), not long after the fluid flow will develop small irregularities (not greater than small particle diameters) at random locations in the cuttings bed. These dispersed irregularities over the bed soon start joining and go through a complex development stage to finally become a fully developed rippled cuttings bed, as shown in figure (12-B). This type of bed configuration normally has triangular shapes in cross section parallel to the fluid flow, and the stronger the cuttings transport rate the faster they will be formed and achieve equilibrium.

If the fluid flow strength is increased, the ripples grow into larger dunes, which are geometrically similar to the ripples but are at least an order of magnitude larger, as seen in figure (12-C).

Further increasing the strength of the fluid flow, a large portion of the cuttings is transported over the dunes as suspended load; hence, the dunes reduce in size and become more rounded until they finally disappear giving way to a nearly planar bed where suspended load and bed load are transported simultaneously, as seen in figure (12-D).

An additional increase in fluid flow strength creates gentle standing waves on the water surface, and the resulting pattern of higher and lower near bed velocity causes the bed to be moulded similarly to the train of waves at the fluid surface, forming anti-dunes, as shown in figure (12-E). Important to mention that the development of anti-dunes is dependent on the presence of free surface, hence, for conduit fluid flow the bed configuration sequence would have stopped at the planar bed stage.

During the formation of ripples, the fluid flow depth is not important because the processes within the viscous sub-layer control this bed configuration, but for all other bed forms (dunes and anti-dunes) the fluid depth is vital, since it controls the scale of the turbulent eddies in the flow that in turn control the height and wavelength of dunes and anti-dunes.

Until now, the effects of cohesive materials have been ignored, but when taken into account they drastically change the cuttings bed configuration time response and profiles. Although studies of this matter are quite rare, Baas (2013) studied the development rate, size and shape of bed configurations in mixed cohesive muddy sands under steady uniform flow conditions. He noticed major differences on the texture, morphological and dynamic properties of the bed configurations.

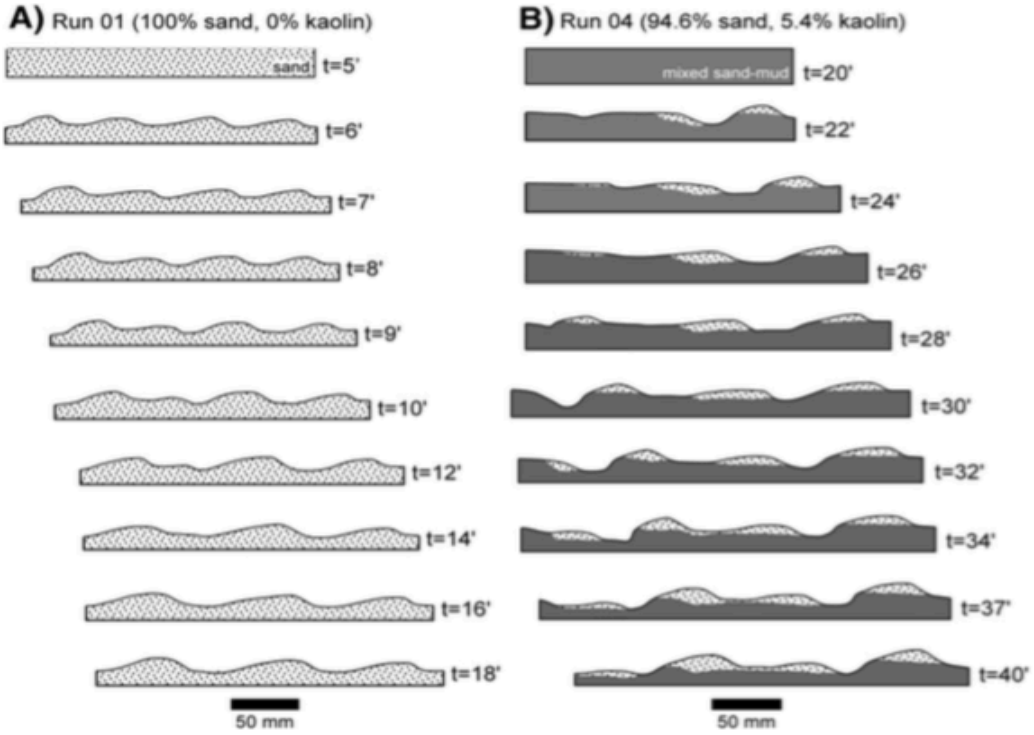

Figure 13: Cuttings bed configuration for: A - 100% sandstone; B - cohesive material added (from Baas, J.H., Davies, A.G., and Malarkey, J., 2013, Bedform development in mixed sand–mud: the contrasting role of cohesive forces in flow and bed)

Figure (13) displays one of the test results obtained by Baas (2013), where he also confirmed that the erosion threshold for cohesive beds is indeed higher and the erosion process was extremely irregular, as scours vary greatly in length and depth.

3.2.3 Cuttings Transport Rate

The transport rate, Q_s, is a measure of the mean mass of cuttings that passes across a given flow transverse cross-section in unit time. For a flume laboratory experiment the cuttings transport rate can be measured through various methods, although here we focus on the screen trap method as shown in figure (14). When installed across the flow, the mass of each of the n particles that passes across the screen in unit time per unit width of the channel represents the unit width transport rate (equation (8)).

$$q_s = \frac{\sum_1^n m_i}{channel\ width} \tag{8}$$

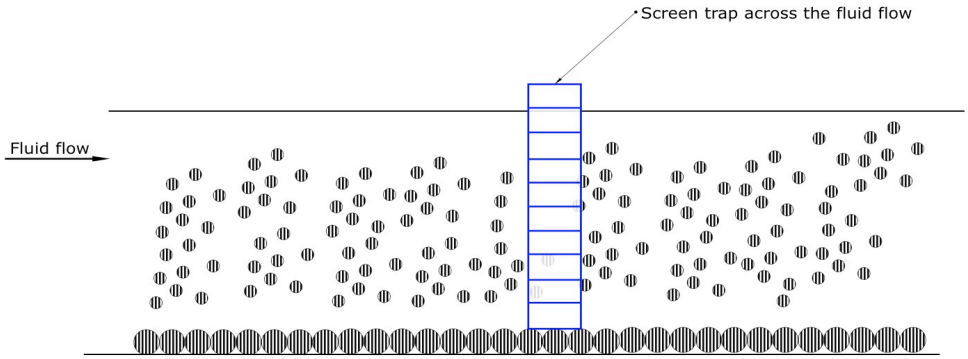

Figure 14: Screen trap

However, regardless of how well designed the trap is, it always affects the flow near the trap to a certain extent (backwater effects), and in cases where rough bed configurations are present, the catch depends strongly upon the trap location relative to the crest (region around the highest point in cuttings bed configuration) and trough's (region around the lowest point in a cuttings bed configuration) of the rough bed. Also, note that the sampling time should be small enough, especially in cuttings recirculating flume experiments, so that deficit in transport does not propagate by recirculation of the sediment back to the trap.

3.2.4 Gradation Independence Vs. Equal Mobility

A good way of looking at this problem is by projecting a laboratory flume experiment. If a nearly perfect well-sorted uni-sized granular cuttings batch is prepared, with sizes raging from coarse to fine sand, and for each size fraction a flume run is performed to evaluate the unit width bed load transport rate, q_b, over a wide range of boundary shear stresses (from very near the threshold to several times above the threshold), the plot of unit width bed load transport rate against the boundary shear stress for each of the cuttings size fractions should resemble the one shown in figure (15).

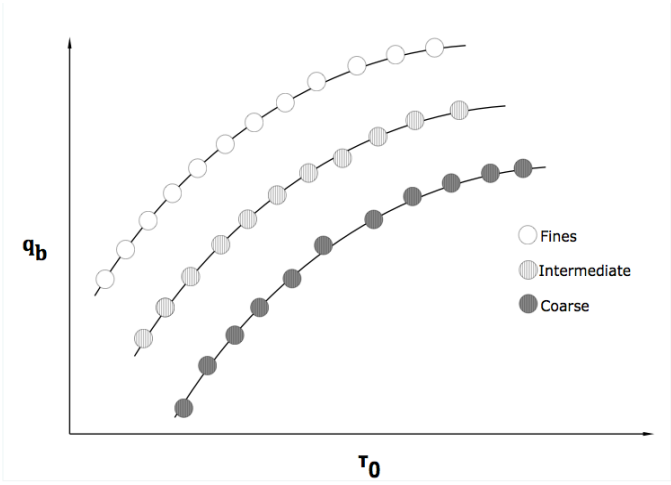

Figure 15: Transport rate vs boundary shear stress for three for 3 granular cuttings size fractions

For each cuttings size fraction, the data points for the runs are expected to fall on an approximately straight line in a log-log plot, with the unit width bed load transport rate increasing steadily with boundary shear stress. The location of the curves in relationship with each other is to be expected, as it is easier to move finer particles than coarser particles.

Now, consider that the flume experiment is done for the mixture of the three particle size fractions together to form a single cuttings batch. The fractional transport rate for each one of the 3 size fractions can be viewed as being the ratio of the transport catch, p_i, over the proportion of the ith size fraction in the bulk cuttings batch placed in the flume, f_i, all multiplied by the unit width transport rate, as shown in equation (9).

$$q_{bi} = \frac{p_i}{f_i} q_b \tag{9}$$

In the case of gradation independence, each of the size fractions being transported is independent of the interaction with the other size fractions, hence the plot results would be 3 curves of q_{bi} vs. τ_0, as shown in figure (16).

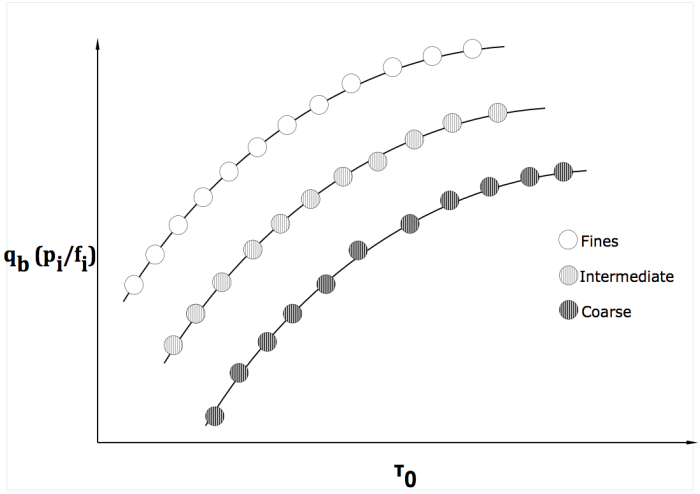

Figure 16: Fractional transport rate vs boundary shear stress for perfect gradation independence scenario

In the case of equal mobility, all of the normalized fractional transport rates are the same for a given boundary shear stress value, meaning that the transport dynamics of the various size fractions are so closely connected that the transport rates of the various size fractions are all the same when adjusted for their proportions in the cuttings bed mixture, as shown in figure (17).

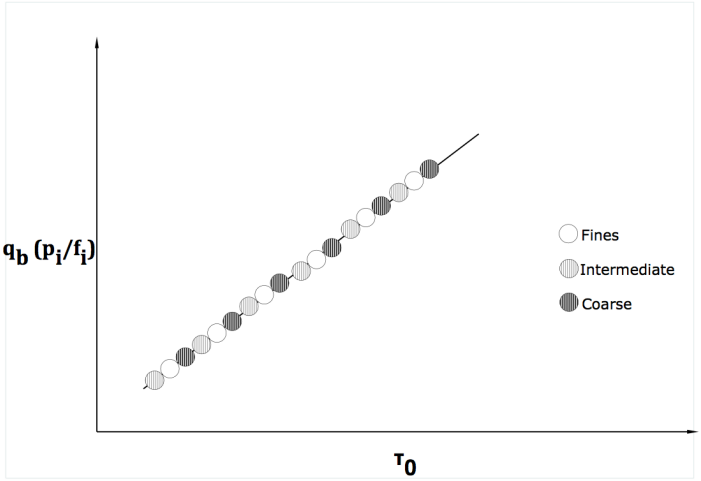

Figure 17: Fractional transport rate vs boundary shear stress for equal mobility scenario

In cases of cuttings feeding flumes, which are the ones that better resemble drilling operations, the condition of equal mobility is forced upon the flume because the flow must transport all the cuttings that are being feed into the system, otherwise the flow and cuttings transport will never achieve an equilibrium state.

Mixed size sediment transport has three events that majorly contribute to the degree of equal mobility transport mechanism scenario:

- Particle weight effect: larger and denser particles are harder to move than smaller light particles.
- Sheltering effect: larger particles are more exposed to the flow, and the smaller particles normally tend to get sheltered by the larger ones.
- "Rollability" effect: lager particles can roll easier over a bed of large particles, while the smaller particles can not move as easily over the same bed.

Sub-chapter 3.4 will make clear how these effects influence the erosion threshold and what is the assumption taken when such constraints emerge.

Again, until now the effects of cohesive particles have not been accounted for. According to the studies performed by Jain (2009), the inclusion of cohesive materials in a granular cuttings bed mainly changed the size of the particles being transported and the modes of cuttings bed transport. He noticed that when 20% of cohesive particles where added, most of the cuttings moved by rolling, and in cases of concentrations above 20% the cuttings where detached from the bed surface in the form of thick flakes. He also noticed that depending on the consolidation time and the flow strength applied, the cuttings were eroded in the form of lumps or chunks of a mixture of cohesive and non-cohesive materials of different shapes and sizes.

3.3 Observing Erosion of a Cuttings Bed

Although the laboratory experiments are focused on the erosion threshold of a cuttings bed, the erosion of a cuttings bed will also be assessed, as it contributes to the overall knowledge on the matter. Figures (18) and (19) provide a good description of what differentiates the erosion process from the erosion threshold of a cuttings bed.

When the fluid flow strength is higher than the gravitational, contact and bonding forces in the active layer of a cuttings bed, selected particles will start getting mobilized, and this process is here characterized as the condition for erosion threshold. Although there is more to be said about this stage (see sub-chapter 3.4) for now this definition is satisfactory.

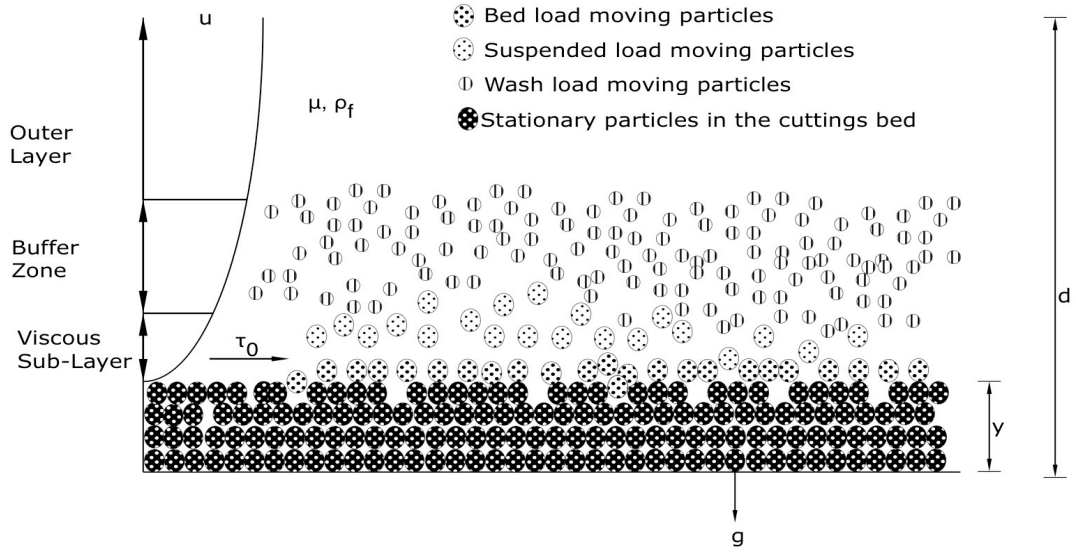

Figure 18: Erosion of a cuttings bed

If the fluid flow strength is sufficiently increased, instead of a selected particle movement, most of the particles within the active layer are suitable to be moved (even though the movement is stochastic due to the various hindering effects mention in the previous sub-chapter), meaning that at a given time there will be a large number of particles in motion, and this is the condition here used to define erosion. Basically if the cuttings load concentration is high enough, one is within the erosion process.

During the erosion of a cuttings bed, the most relevant events one wants to keep track of are:

- How are the particles moving in the flow (modes of particle motion)
- How fast are the particles moving in the flow
- At any given time in the flow, what is the concentration of cuttings in a chosen section of the flow (cuttings load)
- How fast does the flow dispose himself of the particles (cuttings transport rate)

All these events are dependent on a serious of physical quantities, and from what has been discussed until this stage, the next step is to create a link between the events and the physical quantities, helping in the construction of an expression defining the erosion of a cuttings bed process.

As previously discussed in section (3.2.1), one can expect that the modes of particle motion will depend mainly upon:

- Fluid forces on the particles and bed: τ_0, ρ_f, μ
- Particles mean size: D
- Particles mean density: ρ_s

The speed at which the particles are travelling in the flow is expected to depend on:

- Fluid forces on the particles and bed: τ_0, ρ_f, μ
- Particles mean size: D
- Particles mean density: ρ_s
- Where are the particles located in the flow (turbulent diffusion effects on the particles): d,y
- Cuttings bed cohesive strength: %CM (amount of cohesive material), CT (consolidation time)

The cuttings load is expected to be dependent on:

- Fluid forces on the bed and particles: τ_0, ρ_f, μ
- Particles mean density: ρ_s
- Fluid flow depth: d,y
- Cuttings bed cohesive strength: %CM, CT

Finally from what was discussed in sections (3.2.2, 3.2.3 and 3.2.4), the cuttings transport rates is mainly dependent on:

- Fluid forces on the bed and moving particles: τ_0, ρ_f, μ
- Particles mean size: D
- Particles mean density: ρ_s
- Fluid flow depth: d,y
- Cuttings bed configurations: τ_0, ρ_f, μ, d and y (for fluid flow related physical quantities) and, ρ_s, D, λ, %CM and CT (for cuttings bed related physical quantities)
- Cuttings bed sorting: σ
- Cuttings bed cohesive strength: %CM, CT

Noticeably a lot of the variables are repeated, and for the deduction of a model each of the physical quantities only needs to be accounted for once, therefore equation (1) can now be re-written as:

$$Erosion = f\left(\tau_0, \rho_f, \mu, d, D, y, \sigma, \rho_s, \%CM, CT, g\right) \tag{11}$$

3.4 Observing Erosion Threshold of a Cuttings Bed

The condition of incipient particle motion in a cuttings bed is of stochastic nature, and the instantaneous resultant forces on the bed as well as the turbulent velocity vary irregularly with time. At very low fluid flow velocities (well below the threshold of particle movement), some bed particles are moved by the flow because the impact of turbulent eddies on the cuttings bed causes the fluid forces on the sediment particles to vary widely, meaning that even at weak flow strengths a particularly strong turbulent eddy would occasionally cause one or more particles to move.

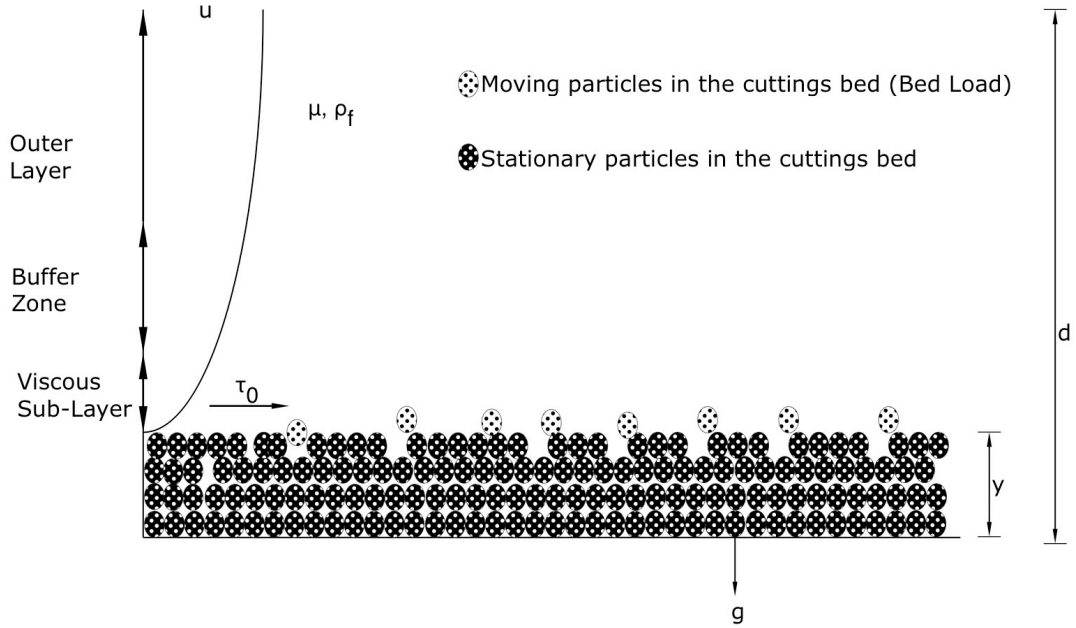

Figure 19: Onset of particle motion in a cuttings bed driven by fluid flow

At this wide range of weak flow strength conditions, particle motion can still be visible, but two important questions arise:

- Is this random and non-uniform motion considered to be the onset of erosion?
- For how long should the particles in the bed be uniformly moving for it to be considered the start of erosion?

This uncertainty in the determination of the erosion threshold is the main reason behind so much scatter in the studies made until date. Following the sedimentology field approach and despite all the uncertainties, the critical shear stress still has a certain physical reality, and there are two main ways of identifying the threshold condition:

- Watch the bed method: this is the most natural method of the defining the threshold condition. The main problem with this method is the wide range of weak particle movement conditions that might be

unreliable. In this method, the flume run is usually set up with an initially planar bed and the bed is watched for signs of particle motion in the planar bed.

- Reference transport rate method: This is the method chosen for this thesis and it bypasses the mentioned uncertainties for incipient particle motion. By measuring the cuttings unit transport rate at various increasing values of fluid flow strength, a plot of q_s vs. τ_0 is obtained. The erosion threshold is then assumed to be the boundary shear stress value at the minimum unit width transport rate. But note that even if the cuttings bed surface is smoothened at the start of every experiment, the tests are usually made after the cuttings transport has come into equilibrium with the flow and there is a large possibility that ripples or other bed configurations have been formed, hence, cuttings bed load movement is affected (cuttings transport rate over a rippled bed is generally different from that over a planar bed of the same sediment experiencing the same flow conditions, so the threshold is identified in a fundamentally different situations).

For non-cohesive granular beds, erosion threshold is normally described through the Shields parameter as shown in equation (12).

$$\tau_c = \theta = \frac{\tau_0}{Dg(\rho_s - \rho_f)} \tag{12}$$

This expression is a non-dimensional form of the boundary shear stress obtained by Shields (1936), which also plotted the resulting data for incipient particle motion from flume experiments on a graph of non–dimensional boundary critical shear stress vs. the boundary Reynolds number (also a non-dimensional expression), giving rise to the shields curve as shown in figure (20). Note also that the reference transport rate method was the one chosen by Shields (1936).

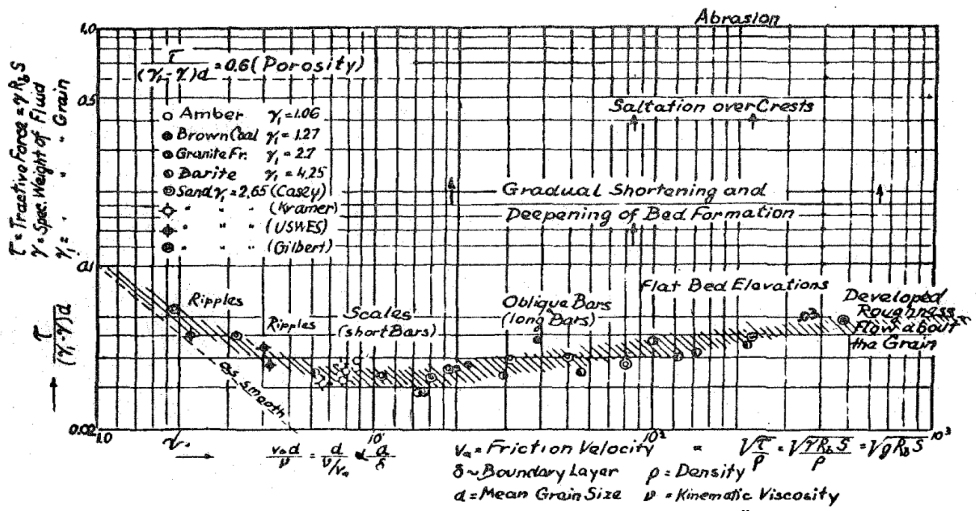

Figure 20: Shields Curve (from Shields, A., "Anwendung der Ähnlichkeitsmechanik und der Turbulenz-forschung auf die Geschiebebewegung," Preussische Versuchsanstalt für Wasserbau und Schi bau Report No. 26, 1936.)

Important to mention at this stage is the debate on the equal mobility condition for the erosion threshold of mixed size cuttings bed (when using the transport rate method). For a well-sorted cuttings bed batch, the critical shear stress proposed by Shields (1936) can be accurately applied by using the mean grain size of the cuttings batch. In cases of poorly sorted cuttings bed, because of the particle weight, sheltering and rollability effects previously mentioned, the mobilization of the particles will only be achieved when the critical shear stress for the coarser particles is achieved. As we will be dealing with fairly well-sorted cuttings for the laboratory experiments, the effects of sorting size will not be accounted for.

Similar to granular beds, researchers agreed that the critical shear stress is a much more favourable parameter to describe the condition of incipient particle motion when cohesion is accounted for, as the critical velocity depends on other hydraulic parameters. Nonetheless, in such cases, Shield's parameter normally seriously underestimates the true critical shear stress of cohesive cuttings bed. As said before, there is no universal correlation relating the cohesive parameters to the threshold of motion, leaving the choice of physical quantities to what best fits the users' experimental purposes. Table (1) shows some of the empirical correlations proposed until date.

Table 1: Empirical correlations for cohesive soil erosion (from Utley, B. C. and Wynn, T.M. (2008). "Cohesive Soil Erosion: Theory and Practice." World Environment and Water Resources Congress 2008: Ahupa'a, May 12, 2008 – May 16, 2008, American Society of Civil Engineers, Honolulu, HI, United States, Environmental and Water Recourses Institute.)

Equation (#)	Soil Property
$\tau_c = 0.16(I_w)^{0.84}$ (3)	I_w = plasticity index
$\tau_c = 10.2(D_r)^{-0.63}$ (4)	D_r = dispersion ratio
$\tau_c = 3.54x10^{-28.1D_{50}}$ (5)	D_{50} = mean particle size (m)
$\tau_c = 0.493x10^{0.0182P_c}$ (6)	P_c = % clay by weight
$\tau_c = 0.1 + 0.18(SC) + 0.002(SC)^2 - 2.34E-5(SC)^3$ (7)	SC = % silt and clay

Now, similar to what has been done in the previous sub-chapter, the main and obvious question for the erosion threshold is:

- When do the particles start moving?

According to the figure (19), one can see that this condition depends on the following physical quantities:

- Fluid forces on the cuttings bed: τ_0, ρ_f, μ
- Cuttings mean size: D
- Particles mean density: ρ_s
- Cohesive strength of cuttings bed: %CM, CT

Note that both the channel flow and cuttings bed heights (d and y respectively) are not accounted for, as the particles at this stage are inside the viscous sub-layer. Therefore, equation (2) can now be re-written as:

$$Erosion\ Threshold = f\left(\tau_0, \rho_f, \mu, D, \rho_s, \%CM, CT, g\right) \tag{13}$$

4 Model Derivation

Equations (11) and (13) provide an understanding of the main physical quantities influencing both erosion and erosion threshold of a cuttings bed. This is extremely important information, but it's still an initial step towards a valuable investigation.

As it stands, taking equation (13) as an example, an enormous amount of experiments are required to link each of the physical quantities to the erosion threshold condition. To overcome this problem, this chapter presents a way of better representing both equations (11) and (13) through the use of dimensional analysis methods, so that more meaningful expressions can be used to understand both conditions.

4.1 Dimensional Analysis

Dimensional analysis is the analysis of the relationships between different physical quantities by identifying their fundamental dimensions and units of measure and tracking these dimensions as calculations or comparisons are made. Their main applications are:

- Check correctness of a physical equation
- Derive relations between different physical quantities involved in a physical phenomenon
- To change from one system of units to another

A physical quantity is a property of a phenomenon (body or substance) that can be quantified by a measurement, and it's normally expressed as a combination of a number and a unit or combination of units (e.g. ρ_{water} = 1kg/m^3). Base quantities are a set of physical quantities that cannot be expressed in terms of other quantities. The list of base quantities as well as their respective dimensions is shown in table (2).

Table 2: Base quantities and their respective dimensions and SI units

Base Quantity	Dimension	SI Units
Length	L	Metre
Mass	M	Kilogram
Time	T	Second
Electric current	I	Ampere
Thermodynamic temperature	Θ	Kelvin
Amount of substance	N	Mole
Luminous intensity	I_v	Candela

4.1.1 Buckingham Pi Theorem

In simplified terms, the Buckingham's Pi theorem states that if there is a physical meaningful equation involving a certain number n of physical variables, then the original equation can be re-written in terms of p = n-k non dimensional parameters, where k is the number of physical dimensions involved.

This is a key theorem for dimensional analysis, as it provides the means for computing sets of non-dimensional parameters from given variables even if the form of the equation remains unknown. Nevertheless, the choice of non-dimensional parameters is not unique (a great variety of them can be created depending on the purposes of the user) and the theorem only provides a way of generating sets of non-dimensional parameters without any remarks to which ones would be more useful.

In a more exhaustive form, Buckingham's pi theorem is seen as:

$$f(q_1, q_2, \dots, q_n) = 0 \tag{14}$$

Where q_i are the n physical variables, and they are expressed in terms of k independent physical units, hence equation (14) can be re-written as:

$$F(\pi_1, \pi_2, \dots, \pi_p) = 0 \tag{15}$$

Where π_i are the dimensionless parameters constructed from q_i by p = n-k non-dimensional equations (the pi groups) of the from:

$$\pi_i = q_1^{a_1} * q_2^{a_2} * \dots q_n^{a_n} \tag{16}$$

4.2 Erosion Threshold Model

Equation (13), gives a good perspective on the main physical quantities influencing the erosion threshold of a cuttings bed, but since the effects of polymeric substances and salt are also to be evaluated, equation (13) is here re-written as:

$$Erosion\ Threshold = \tau_c = f(\tau_0, \rho_f, \mu, D, \rho_s, \%CM, CT, \%PM, \%SM, g) \tag{17}$$

Where %PM and %SM stand for the amount of polymeric and salt material respectively, introduced into the cuttings bed. The variable τ_c is here chosen to describe the erosion threshold condition (the shear stress value needed to initiate particle motion of a certain cuttings bed).

Equation (17) has 11 variables that can be described through 3 basic quantities (mass, length and time), therefore using Buckingham's Pi theorem one should expect to have 8 non-dimensional expressions representing the erosion threshold condition. There are a great deal of forms these 8 non-dimensional

expressions can take, all depending on what better suits the purpose of the study. The full derivation of the expressions is shown in appendix (A.2).

Before presenting the results of the derivations, the variable λ representing the submerged specific weight is here introduced, as shown in equation (18).

$$\lambda = g(\rho_s - \rho_f) \tag{18}$$

So, by turning equation (17) into a non-dimensional expression one obtains:

$$\frac{\tau_c}{\lambda D} = f\left(\frac{\tau_0}{\lambda D}, \frac{\rho_f U^* D}{\mu}, \frac{\rho_s}{\rho_f}, \frac{CT\tau_0}{\mu}, \%CM, \%PM, \%SM\right) \tag{19}$$

The first term in the R.H.S of equation (19) is the already presented shields parameter (see equation (12)) and if the numerator and denominator are multiplied by the particle mean size squared, D^2, it can be viewed as the ratio of fluid forces on the particle to the weight of the particle. The second term is the boundary Reynolds number, which characterizes the nature of the flow near the boundary. The variable U^* is known as the shear velocity and its normally expressed as:

$$U^* = \sqrt[2]{\frac{\tau_0}{\rho_f}} \tag{20}$$

The effects of density ratio (relative inertia) are accounted for with the third term in equation (19), and the fourth term should account for the effects of the consolidation time. The last three terms (%CM, %PM and %SM) did not change from the previous equation because they already are non-dimensional. Equation (19) is then the proposed expression to study the erosion threshold problem through laboratory experiments (which will be appropriately explained in chapter 5).

4.3 Erosion of a Cuttings Bed Model

The same approach taken for the model deduction of the erosion threshold of a cuttings bed can be applied for the erosion model, although the specifications on how the non-dimensional expressions are obtained is not here discussed.

Equation (11) can then be viewed as:

$$Erosion = f\left(\frac{\tau_0}{\lambda D}, \frac{\rho_f U^* D}{\mu}, \frac{d_f}{D}, \frac{\sigma}{D}, \frac{\rho_s}{\rho_f}, \%CM, \frac{CT\tau_0}{\mu}, \%PM, \%SM\right) \tag{21}$$

There are two new non-dimensional expression introduced in the R.H.S of equation (21). The first one is the relative roughness (d_f/D), where d_f represents the actual fluid flow depth (d_f = d-y). In cases where the fluid depth is much higher than the particles mean size this can be ignored. The second new expression is the sorting to size ratio, represented by σ/D, and in cases of well-sorted cuttings it can also be omitted from the expression.

5 Laboratory Test

A simple rectangular cross section flume laboratory set up is here chosen to conduct the experiments and this set up has been purposely chosen so that a single person can easily run it. A full description of the test matrix and procedures needed to conduct the experiments are also here presented.

5.1 Lab Set Up

The full flow loop schematics in shown in figure (21). An overhead tank where the chosen drilling fluid is stored is connected to a vertical feed pipe, which is made long enough so that the required flow rates can be achieved through hydrostatic gravity energy. The calculations for the required height of the vertical feed pipe are given in the appendix A.1.

At the inlet of the horizontal section and just ahead of the test tray, an on/off valve, a flow control valve to adjust the fluid flow rates to desired values, and a dump valve to divert the fluid flow if necessary are installed as shown in figure (21). To ensure that at the entrance of the test tray section the flow is fully developed, a 50 cm flow developing test section is connected to the actual test tray section, as shown in figure (22). Both flow developing sections and test tray sections have an 8 cm width, and a 50 cm walls height. The walls of the flume are transparent for visual monitoring purposes.

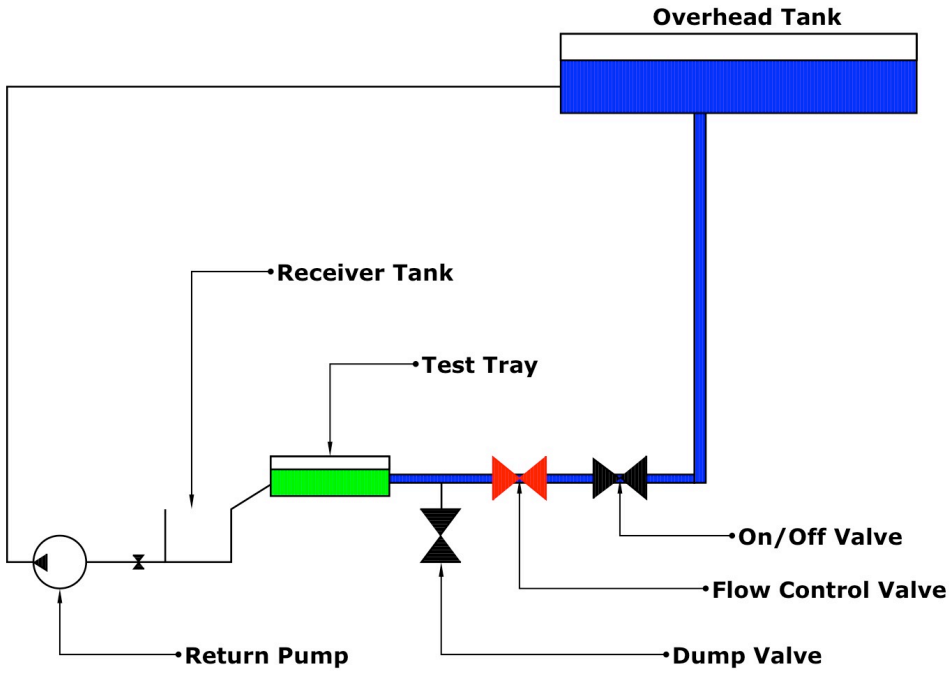

Figure 21: Laboratory set up schematics

To further reduce the swirls and non-symmetry in the fluid flow at the test section, a flow conditioner is also installed. The designed flow conditioner has the following characteristics:

- Orifice diameter = 6mm
- Flow conditioner length (thickness) = 10mm

This design follows the basic guidelines, with the length 1.7 times the diameter of the holes, although a really efficient flow conditioner design requires much more work on the matter. Nonetheless, this will help improve the reliability of the tests, because for every test run the fluid flow profile across the test section will remain consistent, helping reduce uncertainties. The test tray section is 60 cm long and the test section is 40 cm long. Also, during the experiments an inlet and outlet weirs are placed (10 cm long each), as seen in figure (22), so that entrance and exit effects of the fluid flow are reduced. At the end of the test tray is the collecting tank that is connected to a pump that sends the fluid back to the overhead tank restarting the fluid flow loop.

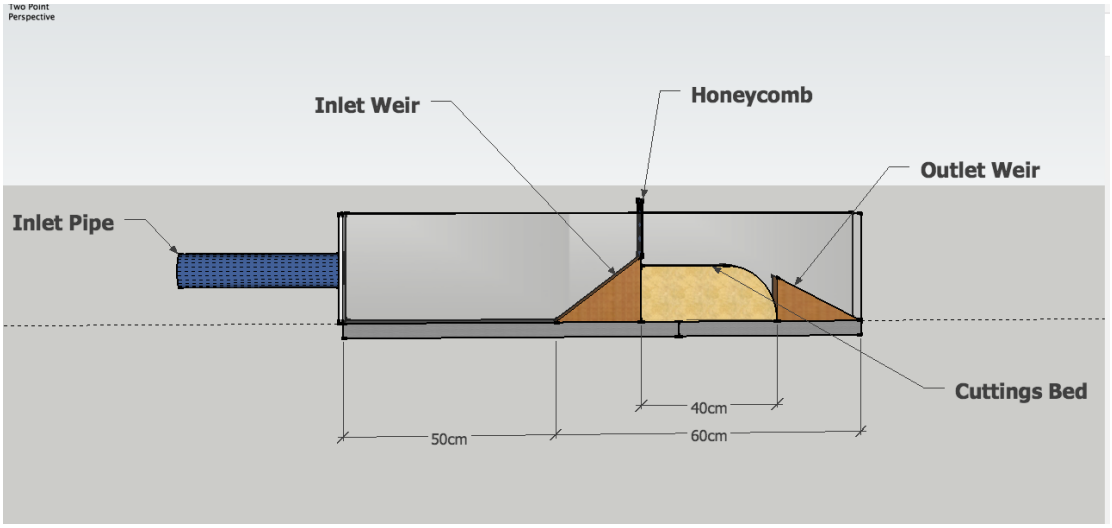

Figure 22: Flume design

5.2 Test Materials

The experiments are based on the theory presented in chapter 3 and the model proposed in chapter 4, where the considerations about the main physical quantities and non-dimensional expressions surrounding the onset of particle motion are presented.

Here we divide the materials into two boundaries (fluids and cuttings bed composition) and the main physical quantities describing them are also presented, as seen in tables (3) and (4).

Fluids properties are accounted for by taking the influence of the fluid density, viscosity and boundary shear stress, where the latter can be evaluated with the use of equation (5).

Table 3: Test drilling fluids

Drilling fluid	Fluid composition	Density	Viscosity
[]	[]	[Kg/m^3]	[Pa.s]
WBM	Water	1000	0.001
OBM	Paraffin (Exxon 60D)	800	0.007

For the cuttings bed composition, the density, particle average size and the amount of cuttings and added additives are presented below.

Table 4: Sandstone cuttings bed and additives main properties

Material Type	Specific Density	Mean Particle Size	Typical Concentrations	Number of Variations	Total Number of Cuttings Bed
[]	[Kg//l]	[μm]	%	[]	[]
Sandstone	2.65	Coarse sand (500 to 1000)	100, 90,80, 75, 70 and 65	6	9
Barite	4.5	3 to 74	10,20	2	
Bentonite	0.801 to 0.961	<2	10,15,20	3	
Polymer		<2	5,10	2	
Salt	2.03		5	1	

Sandstone is here used as the main composition for the cuttings bed and all other materials are the chosen cuttings additives. Barite as an inert solid is here used to investigate the effects of density ratio, bentonite particles are used to unveil the effects of cohesive materials into the cuttings mix, polymers for the influence of polymeric substances and finally the effects of electrolytes into the cuttings mix is done with the use of salt additives.

5.3 Test Matrix

Now that the laboratory set up and all test materials are known, the full test matrix can be determined.

The first step is to create a reference point for the experiments by studying the erosion threshold of a cuttings bed on a 100% well-sorted coarse sandstone cuttings. The next step is to evaluate the effects of barite additives in to the cuttings bed mix, and this will help in the understanding of the effects of relative inertia (since barite is so much denser than sandstone). For this stage the following cuttings bed compositions are prepared:

- 90% well–sorted coarse sandstone cuttings mixed with 10% barite
- 80% well-sorted coarse sandstone cuttings mixed with 20% barite

For all the cuttings bed compositions mentioned above, because there's no cohesive materials added, they are left to rest in the test fluid for a period of time of 1 hour (no variations in CT for non-cohesive beds).

The next parameter to be evaluated is the effects of cohesive material in the erosion threshold and this is achieved by steadily increasing the percentage of bentonite additives into the cuttings bed composition. For this set of cuttings, tests should be performed for 3 different CT's (see table (5)), and the cuttings composition should be as follows:

- 80% well-sorted coarse sandstone mixed with 10% barite and 10% bentonite
- 75% well-sorted coarse sandstone mixed with 10% barite and 15% bentonite
- 70% well-sorted coarse sandstone mixed with 10% barite and 20% bentonite

The effects of polymeric additives into the cohesive bed will be accounted for through the following cuttings bed compositions:

- 75% well-sorted coarse sandstone mixed with 10% barite, 10% bentonite and 5% polymer
- 70% well-sorted coarse sandstone mixed with 10% barite, 10% bentonite and 10% polymer

This set of cuttings bed compositions will also be tested under 3 different consolidation times.

Finally the effects of salt additives are tested with a cuttings bed composed of 65% well-sorted sandstone mixed with 10% barite, 10% bentonite, 10% polymer and 5% salt. This cuttings bed composition will also be tested for 3 different consolidation times.

Recall that it is the reference transport rate method that will be used here, hence, from a reference "critical" flow rate (that can be converted to boundary shear stress using equation 3) plus 7 other higher chosen flow rates, the bed load transport rates are measured for each of the cuttings bed compositions mentioned above. This will provide relationships between the unit width transport rate and boundary shear stress (recall section 3.8), which in turn can be used to evaluate the cuttings bed erosion threshold values, by extrapolating the graphs to a value of a minimum reference transport rate. Once those are obtained, plots of the non-dimensional critical shear stress against the respective non-dimensional expressions of interest (boundary Reynolds number, density ratio, etc.) can be obtained, hence, any differences in the values of the erosion threshold for both drilling fluids can be fully analysed. Table (5) shows a summary of the test matrix and the total number of tests to be conducted.

Table 5: Test matrix and total number of test

Variable	N-o of variations	Specifications	Total Number of Tests
Cuttings bed composition	9	See table 4	(3*2)+(6*4*2) = 54
Cuttings resting time	4	Always 1 hour + three selected variations of 5, 10 and 24 hours	
Flow rate	8	The chosen incipient particle motion fluid flow rate + 7 other higher flow rates	
Drilling Fluid	2	See table 3	

5.4 Test Procedure

To ensure quality of experiments and the data gathered, an appropriate workflow is prepared. The first point to be dealt with is the cuttings bed treatment; figure (23) shows the test section during the cuttings treatment phase. During this stage, the section should be slightly tilted to the vertical and the block at the end of the section should also be positioned so that the cuttings bed profile seen in figure (23) can be achieved. To ensure that the active layer of the cuttings bed contains the additives of interest, for all cuttings with additives a bottom layer made of only sandstone should be laid down first, leaving 30% of sandstone mixed with the percentage of additives in question to be added at the top of the already laid layer (see figure (24)).

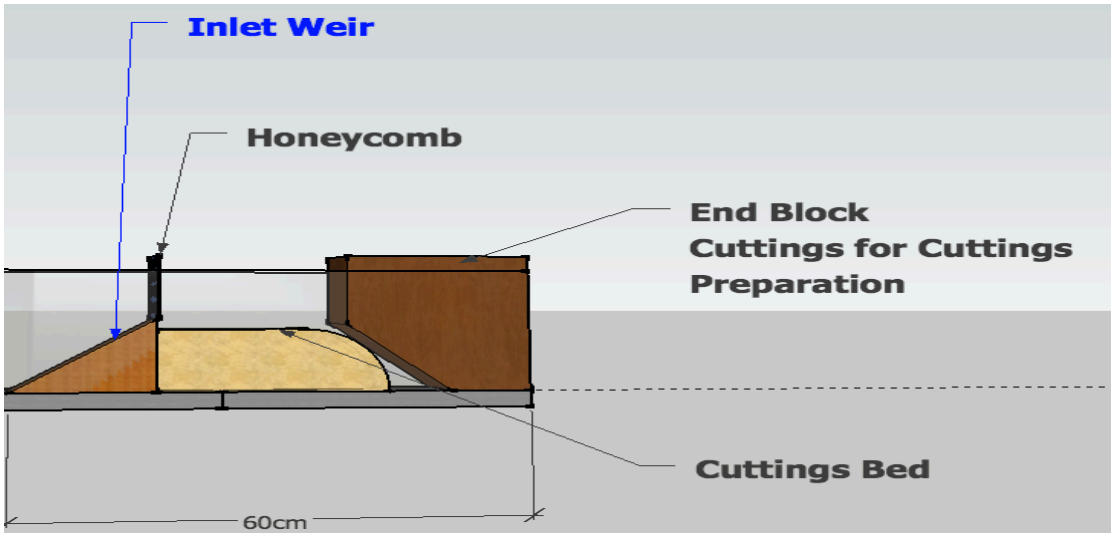

Figure 23: Cuttings bed preparation

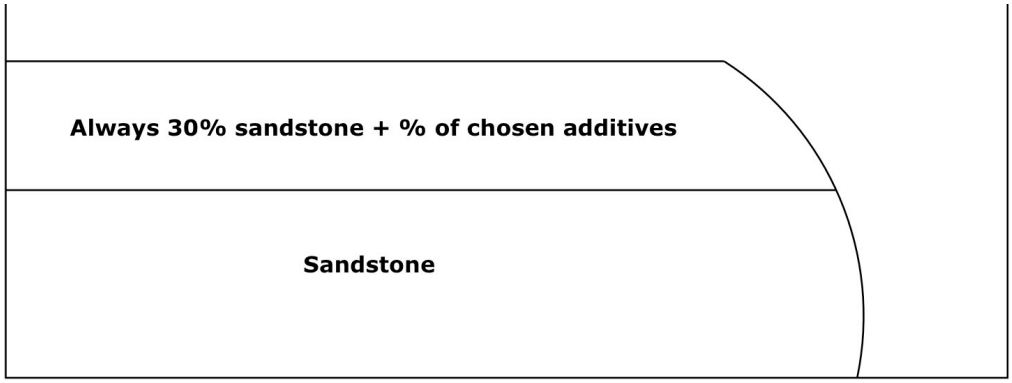

Figure 24: Cuttings bed composition set up

Also, for consistency in every test, after the cuttings beds are allowed to rest, they should be levelled so that a smooth surface is created. The workflow to be followed during the experiments is presented in table (6).

Table 6: Test procedure

Test Procedure		
Fluid Flow Check	Cuttings treatment	Test run and Data Collection
Fill feed pipe with fluid and close ball valve	Place the blocks at both ends of test tray (as shown in figure (23)) and fill in the test section of the tray with 1 l of the fluid to be tested	Open ball valve and slowly increase the flow rate until the desired onset of particle motion is obtained.
Set flow rate to a small desirable value by adjusting the flow control valve	Place 1 l of test material (cuttings +additives) in test section of the tray and let it settle	Slowly increase the flow rate in steps and at 7 other higher chosen flow rates place the screen trap (x centimetres away from the start of the test section and y centimetres in height from the bed) so that the transport rates over a 10 second period can be obtained

The main events one wants to monitor during the experiments and how to do so are also here described:

- Modes and speeds of particle movement: These can be tracked using video recording techniques, so that the process can be sped up or slowed down at will to better understand the nature of particle motion
- Cuttings bed geometry: Again, video recording is very useful, as the different cuttings bed configurations can be tracked over time

- Cuttings transport rate: Placement of traps across the fluid flow width is the method here chosen. The exact placement of the trap should be reviewed during the experiments.

6 Conclusions and Further Work

In conclusion, although it still needs to be tested, the model here proposed offers a new way to access the efficiency of OBM compared to WBM during the erosion threshold of a cuttings bed. If the methodology proposed to conduct the laboratory experiments is followed, the plots of the non-dimensional shear stress against the 8 non-dimensional expressions (see equation (19)) should provide enough relationships so that the behaviour of both base fluids can be better understood.

Furthermore, this study can be improved and better fitted to drilling operations in horizontal wells with the following considerations:

- Perform erosion and erosion threshold experiments in circular piped flow with cuttings feeding system: Instead of manually preparing the cuttings bed at each test run, the experiments should follow a more realistic approach where the cuttings are feed into the system, but in such cases, the smothering of the cuttings bed at the start of every experiment run cannot be performed, adding an extra level of uncertainty to the problem
- The use of more realistic drilling fluids: The inclusion of additives into the drilling fluid will have to be accounted for. Here, non-Newtonian fluids play a major role, adding an extra level of complexity to the matter
- Broaden the study to limestone and shale cuttings beds: Different type of cuttings should exhibit different erosion and erosion threshold behaviours, hence, those need to be carefully evaluated as well
- Include the effects of specific events normally seen during drilling operations: Drill pipe rotation is a good example of such an event, and it is known to have a significant effect on the cuttings transport during drilling operations

.

7 Nomenclature

g	Acceleration of gravity (m/s^2)
ρ_f	Fluid density (kg/m^3)
ρ_s	Cuttings mean density (kg/m^3)
μ	Fluid viscosity (cP)
τ	Shear stress (Pa)
τ_0	Boundary shear stress (Pa)
y	Boundary height (m)
Θ	Channel slope (^{o})
γ	Fluid specific weight (kg/m^2s^2)
b	Channel width (m)
d	Channel height (m)
u	Velocity (m/s)
D	Particle mean size (m)
σ	Cuttings sorting (m)
q_s	Unit width transport rate (kg/m^2s)
q_b	Unit width bed load transport rate (kg/m^2s)
m_i	Mass of ith cuttings size fraction (m)
q_{bi}	Unit width transport rate for the ith size fraction (kg/m^2s)
p_i	proportion of the transport rate for the ith size fraction (%)
f_i	proportion of the ith size fraction in the bulk cuttings (%)
CT	Consolidation time (h)
%CM	Amount of cohesive material (%)
%PM	Amount of polymeric material (%)
%SM	Amount of Salt (%)
d_f	Fluid flow height above the boundary (m)
λ	Specific submerged weight of the particle (kg/m^2s^2)

8 References

A. Hong, M. Tao, and A. Kudrolli, Onset of erosion of a granular bed in a channel driven by fluid flow, Phys. Fluids **27**, 013301 (2015).

Adari, R. B., Miska, S., Kuru, E., Bern, P., & Saasen, A. (2000, January 1). Selecting Drilling Fluid Properties and Flow Rates For Effective Hole Cleaning in High-Angle and Horizontal Wells. Society of Petroleum Engineers. doi:10.2118/63050-MS .

Baas, J.H., Davies, A.G., and Malarkey, J., 2013, Bedform development in mixed sand–mud: the contrasting role of cohesive forces in flow and bed: Geomorphology, v. 182, p. 19–32..

Buckingham, E. (1914). "On physically similar systems; illustrations of the use of dimensional equations". *Physical Review* **4** (4): 345–376.

Bridge, J. S. (2003). Rivers and floodplains: Forms, processes, and sedimentary record. Oxford, UK: Blackwell Pub.

Heinzen, R. T. (1976). *Erodibility Criteria for Soil.* MS thesis, University of CA, Davis.

Jain, R. K., and U. C. Kothyari (2009), Cohesion influences on erosion and bed load transport, Water Resour. Res., 45, W06410.

Nance, W. B., Muncy, D. D., Garrett, M. M., Gault, A. D., & Kortlang, W. F. (1983, January 1). A Comparative Analysis of Drilling Results Obtained With Oil Mud vs. Water-Base Mud at High Island Block A-270. Society of Petroleum Engineers. doi:10.2118/11357-MS

Ramadan, A., Skalle, P., Johansen, S. T., Svein, J., & Saasen, A. (2001). Mechanistic model for cuttings removal from solid bed in inclined channels. *Journal of Petroleum Science and Engineering*, *30*(3), 129-141.

Shields, A., "Anwendung der Ähnlichkeitsmechanik und der Turbulenz-forschung auf die Geschiebebewegung," Preussische Versuchsanstalt für Wasserbau und Schi bau Report No. 26, 1936.

Southard, John. *12.090 Special Topics: An Introduction to Fluid Motions, Sediment Transport, and Current-generated Sedimentary Structures, Fall 2006*. (MIT OpenCourseWare: Massachusetts Institute of Technology).

Utley, B. C. and Wynn, T.M. (2008). "Cohesive Soil Erosion: Theory and Practice." World Environment and Water Resources Congress 2008: Ahupa'a, May 12, 2008 – May 16, 2008, American Society of Civil Engineers, Honolulu, HI, United States, Environmental and Water Recourses Institute.

Appendix A

A.1 Laboratory Set Up Calculations

To ensure that the required fluid flow rates can be achieved during testing, and because the fluid is not being pumped from the overhead tank, the l-shaped pipe should have a minimum height prerequisite. This is obtained by relating both static and dynamic forces of the testing fluid to meet the condition of an N_{Re} > 2000.

Static forces are described through the potential energy of the fluid, hence:

$$PE = \rho g h \tag{22}$$

Dynamic forces can be described through the kinetic energy relationship:

$$KE = \frac{\rho v^2}{2} + friction\ losses \tag{23}$$

Here we do not take into account the friction losses. Also important to recall, is the expression for Reynolds number, which is given by:

$$N_{Re} = \frac{\rho v d}{\mu_{effective}} \tag{24}$$

The table below provides the minimum heights needed to meet the presented requirements. Two cases are presented, but its just a means for comparison, note that, only one case will be chosen.

Table 7: Hydrostatic head calculations

Base fluid	Reynolds number	μ	ρ	ρ	Feed Pipe Diameter	g	Fluid Velocity	Feed Pipe Height
[]	[]	[Pa.s]	[ppg]	[kg/m^3]	[m]	[m/s^2]	[m/s]	[m]
Water	10000	0.001	8.345	1000	0.088	9.81	0.1136	0.0007
Exon 60D	10000	0.007	6.676	800	0.088	9.91	0.9943	0.050

For the volumetric flow rate**:**

$$q = V/t \tag{25}$$

A.2 Dimensional Analysis

$$\tau_c = f(\tau_0, \rho_f, \mu, D, \rho_s, \%CM, CT, g) \tag{26}$$

For the non- dimensional expression of τ_c and τ_0 by taking λ, μ and D as the repeatable variables:

$$\left(\frac{M}{LT^2}\right)^1 * \left(\frac{M}{L^2T^2}\right)^a * \left(\frac{M}{LT}\right)^b * (L)^c = M^0L^0T^0 \tag{27}$$

By equating the coefficients of M, L and T:

$$M: 1 + a + b = 0 \tag{28}$$

$$L: -1 - 2a - b - c = 0 \tag{29}$$

$$T: -2 - 2a - b = 0 \tag{30}$$

This gives rise to a=-1, b=0 and c=-1, therefore:

$$\left(\frac{M}{LT^2}\right)^1 * \left(\frac{M}{L^2T^2}\right)^1 * \left(\frac{M}{LT}\right)^0 * (L)^{-1} = \frac{\tau_c}{\lambda D} \tag{31}$$

And:

$$\left(\frac{M}{LT^2}\right)^1 * \left(\frac{M}{L^2T^2}\right)^1 * \left(\frac{M}{LT}\right)^0 * (L)^{-1} = \frac{\tau_0}{\lambda D} \tag{32}$$

For the non-dimensional form of $1/\mu$ by taking ρ_f, τ_0 and D as the repeated variables:

$$\left(\frac{M}{LT}\right)^{-1} * \left(\frac{M}{L^3}\right)^a * \left(\frac{M}{LT^2}\right)^b * (L)^c = M^0L^0T^0 \tag{33}$$

Equating the basic dimensions gives rise to a = b =1/2 and c=1, hence:

$$\frac{\rho_f U^* D}{\mu} \tag{34}$$

For the non-dimensional form of ρ_s by taking τ_0, ρ_f and D as the repeated variables:

$$\left(\frac{M}{LT}\right)^{-1} * \left(\frac{M}{L^3}\right)^{1/2} * \left(\frac{M}{LT^2}\right)^{1/2} * (L)^1 = \frac{\sqrt[2]{\rho_f \tau_0} * D}{\mu} \tag{34}$$

By multiplying the numerator and denominator by $\sqrt{\rho_f}$:

$$\left(\frac{M}{L}\right)^1 * \left(\frac{M}{LT^2}\right)^a * \left(\frac{M}{L^3}\right)^b * (L)^c = M^0L^0T^0 \quad (36)$$

Equating the basic dimensions gives rise to a = c = 0and b = -1, hence:

$$\left(\frac{M}{L^3}\right)^1 * \left(\frac{M}{LT^2}\right)^0 * \left(\frac{M}{L^3}\right)^{-1} * (L)^0 = \frac{\rho_s}{\rho_f} \quad (37)$$

For the non-dimensional form of CT by taking λ, 1/μ and τ_0 as the repeated variables:

$$(T)^1 * \left(\frac{M}{L^2T^2}\right)^a * \left(\frac{M}{LT}\right)^{-b} * \left(\frac{M}{LT^2}\right)^c = M^0L^0T^0 \quad (38)$$

Equating the basic dimensions gives rise to a = 0, b = -1 and c=1, hence:

$$(T)^1 * \left(\frac{M}{L^2T^2}\right)^0 * \left(\frac{M}{LT}\right)^{-1} * \left(\frac{M}{LT^2}\right)^1 = \frac{CT\tau_0}{\mu} \quad (39)$$